



# Artifacts resembling Ediacaran or Cambrian fossils: how to identify them and avoid their generation

Thiago F. Toniolo<sup>1</sup>, Juliana M. Leme<sup>1</sup>, Dermeval A. Carmo<sup>2</sup>, Thomas R. Fairchild<sup>1</sup>, Luana Morais<sup>3</sup>, and  
Ricardo I. F. Trindade<sup>3</sup>

<sup>1</sup>Institute of Geosciences, University of São Paulo, São Paulo, 05508-080, Brazil

<sup>2</sup>Institute de Geosciences, University of Brasília, Brasília, 70910-900, Brazil

<sup>3</sup>Institute of Astronomy, Geophysics and Atmospheric Sciences,  
University of São Paulo, São Paulo, 05508-090, Brazil

**Correspondence:** Thiago F. Toniolo (thiago.freitas.toniolo@gmail.com)

Received: 24 March 2023 – Revised: 28 June 2023 – Accepted: 7 July 2023 – Published: 18 August 2023

**Abstract.** The generation of artifacts during sample preparation must be considered in paleobiological studies, particularly during the Ediacaran and Cambrian, since such artifacts can assume forms similar to those of cloudinids and other problematic taxa commonly described in samples from these systems. Chemical reactions between hydrogen peroxide and sulfides from the samples can lead to the formation of tubular and vase-shaped structures. The visual description alone does not allow a conclusion about whether their origin is organic or inorganic. In these cases, chemical composition and ultrastructure analysis are tools that help to distinguish artifacts from bona fide fossils. Scanning electron microscopy can be successfully employed to characterize and differentiate fossils from artifacts. The presence or absence of these structures in thin sections is also an essential piece of information to discuss their biogenicity. Furthermore, not using hydrogen peroxide avoids the risk of formation of the artifacts described here.

## 1 Introduction

Hydrogen peroxide is widely used in the preparation of mineralized microfossils (e.g., Thomas and Murney, 1985; Denezine et al., 2022), which is mainly due the following aspects: (I) efficiency – the oxidation of the organic matter disseminated in the host rock and the heat generated during this reaction propitiate the disaggregation of the sedimentary rock; (II) low toxicity – hydrogen peroxide is metastable and, when it decomposes, does not leave persistent toxic residues; and (III) low cost and accessibility (Thomas and Murney, 1985). However, the use of this reagent also has a drawback: it may lead to the formation of artifacts, particularly in samples with abundant pyrite (Richardson et al., 1973).

Wetzel (1959, 1961, 1967) reported the occurrence of microfossils with granular walls, a white to brown color, a tubular shape and annulations in their external wall in rocks from the Jurassic (Germany) and Cretaceous (Baltic). These tubes present constant or variable diameters and open terminations

at one or both ends. These structures were described as a taxonomic group *incertae sedis* called Anellotubulata.

McLachlan (1973) described occurrences of Anellotubulata in Permian rocks of South Africa (Karoo basin) in addition to suggesting its possible occurrence in rocks from the Permian to Cretaceous of Australia. These tubes were found in samples of disparate facies, such as organic shales, glauconitic and sideritic sediments, sandstones, and limestones rich in organic matter.

McLachlan (1973) described the anellotubulates found in the Karoo basin as being composed of a body chamber and one or more calyces; the body chamber would have an irregular shape and size ranging from 20 and 450 µm, while the calyx would be tubular or horn-shaped, with an open distal end and an external diameter ranging from 10 to 150 µm. McLachlan (1973) also reported that the dimensions of these anellotubulates are not related to the granulometry of the sample, with large tubes occurring in both shales and sandstones.

Electron microprobe analyses conducted by McLachlan (1973) revealed that the anellotubulates were composed of iron and phosphorus, and X-ray diffractometry showed that they do not have a crystalline structure. McLachlan (1973), however, did not provide any explanation about how a fossil with mineralized walls can have neither a crystalline structure nor a conventional composition (i.e., calcite, apatite, opal, etc.).

Richardson et al. (1973) and Pickett and Scheibnerová (1974), puzzled by the various inconsistencies involving the anellotubulates, proposed that these tubes were actually inorganic in origin, having been formed during sample preparation. This would explain the enormous stratigraphic and paleogeographic distribution of these tubular forms (Wetzel, 1967; McLachlan, 1973), as well as their occurrence in the most diverse paleoenvironments and also the amorphous structure of their walls (McLachlan, 1973).

Richardson et al. (1973) placed shale fragments containing disseminated pyrite in a watch-glass with hydrogen peroxide 100 vol. and observed, under the binocular microscope, the formation of streams of bubbles on the surface of the shale. In an interval of a few minutes to a few hours, an initially transparent to white material was deposited along the streams of bubbles, and the diameter of these tubes was proportional to the size of the bubbles. Pickett and Scheibnerová (1974) observed the reaction between crushed pyrite grains of non-sedimentary origin and commercial hydrogen peroxide and came to conclusions similar to those of Richardson et al. (1973).

According to Richardson et al. (1973), the oxidation of pyrite would release the iron that would be incorporated into the tubes. The commercial hydrogen peroxide, which contains phosphate in its composition (it acts as a stabilizer), would be the source of phosphorus, which is also present in these artifacts, thus explaining the presence of these elements in the anellotubulates, as detected by McLachlan (1973).

In samples of gray limestones from the Tamengo Formation and samples of siltstones from the Guaicurus Formation (Corumbá Group, central-western Brazil), tubular objects were found after treatment with hydrogen peroxide (this work). The optical description of the morphology of these tubes was not conclusive regarding whether they were of biological origin or not. After finding in the literature that similar objects could form through the reaction of pyrite with hydrogen peroxide (Richardson et al., 1973; Pickett and Scheibnerová, 1974), this hypothesis was considered. To confirm it, the following procedures were adopted: (I) look for these tubes in thin sections, (II) analyze the composition of the tubes, and (III) repeat the treatment of the samples without using hydrogen peroxide. The results obtained are presented and discussed hereafter, and they attest to the inorganic origin of these tubular objects.

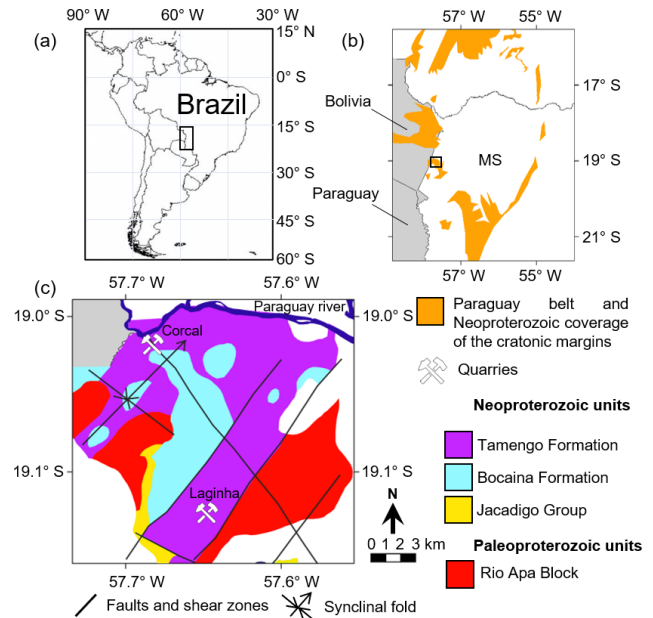


**Figure 1.** Location and geologic setting of study area. (a) South American geographic map. The rectangle indicates the location of the map in (b). (b) Western portion of Mato Grosso do Sul state (MS) with square indicating the location of the map in (c). (c) Geological map of the study area. The geological data were provided by Lacerda-Filho et al. (2006).

## 2 Study area

The study area is located in the western part of the state of Mato Grosso do Sul (Brazil, Fig. 1) and is part of the southern Paraguay Belt, an orogen composed of Neoproterozoic metasedimentary rocks deformed mainly during the Cambrian in the context of collision between the Amazon, São Francisco, Rio Apa, and Paranapanema cratons (Campanha et al., 2011).

This region is characterized by rocks of the Corumbá Group, constituted, from base to top, by the Cadiueus, Cerradinho, Bocaina, Tamengo and Guaicurus formations (Boggiani et al., 2010). The Cadiueus and Cerradinho formations correspond mainly to terrigenous sediments, deposited in a continental context, while the Bocaina Formation is formed by dolomites, phosphorites and shales (Campanha et al., 2011; Morais et al., 2021).

The Tamengo Formation is predominantly composed of dark-gray limestones (grainstones, wackestones and mudstones) and reddish to ochre siltstones and shales (Amorim et al., 2020). This unit contains fossils of *Cloudina*, *Corumbella wernerii*, *Paraconularia ediacarensis*, macroalgae and ichnofossils (Gaucher et al., 2003; Adorno et al., 2017; Parry et al., 2017; Diniz et al., 2021; Leme et al., 2022). The main exposures of the Tamengo Formation are located on the right bank of the Paraguai River between Corumbá and Ladário in the Corcal quarry and in the Laginha quarry (Boggiani et al.,

2010; Fig. 1c). In the Corcal quarry, volcanic zircons provide U–Pb ages of  $542.27 \pm 0.38$  and  $541.85 \pm 0.75$  Myr (Parry et al., 2017). In the Laginha quarry, there is contact between the Tamengo and the Guaicurus formations, with the latter being characterized by a pack of grayish siltstone with a total thickness of about 40 m (Amorim et al., 2020) and sparse occurrences of the macroalga fossil *Eoholynia corumbensis* (Gaucher et al., 2003).

### 3 Methods

A total of 64 samples were collected with stratigraphical positioning along the geological section of the Laginha quarry, with 59 having been collected from the Tamengo Formation and 5 having been collected from the Guaicurus Formation (Fig. 2). At the level of interbedded wackestones and mudstones, between 70 and 82 m, samples were collected at every lithofacies change; for this reason, this level was more densely sampled. Sampling between 130 and 150 m was not possible due to safety issues. Each sample received a code consisting of three letters that refer to the locality of collection and a number with two decimal places that refers to its stratigraphic position. For example, sample LAG 62.60 was collected at the level of 62.60 m of the stratigraphic column of the Laginha quarry.

At the Institute of Geosciences of the University of São Paulo (USP), 36 of the 64 samples were selected for petrographic analysis in order to detail the description of each of the lithofacies of both formations. Then, all 64 collected samples were subjected to disaggregation according to the following steps:

1. Crush until obtaining fragments of approximately  $2 \times 2 \times 2$  cm.
2. In the fume hood, place 200 g of these fragments in a beaker and add 100 mL of commercial  $H_2O_2$  (minimum concentration of 29 %) diluted in 100 mL of deionized water. Leave to react for 7 d. This long reaction time was adopted to optimize the disaggregation of very hard limestones with practically no porosity.
3. Pour the beaker contents into a set of sieves with meshes of 4 mm, 600  $\mu$ m, 250  $\mu$ m, 100  $\mu$ m and 53  $\mu$ m. Sieve with running water.
4. Collect the material retained in each granulometric fraction and place it in an oven at 60 °C until completely dry.
5. Analyze all the seized material under a stereoscopic microscope with a reflected light source, identifying and describing all the structures.
6. Perform digital microphotography of selected objects using a stereoscopic microscope (Olympus DSX 110) with a reflected light source.

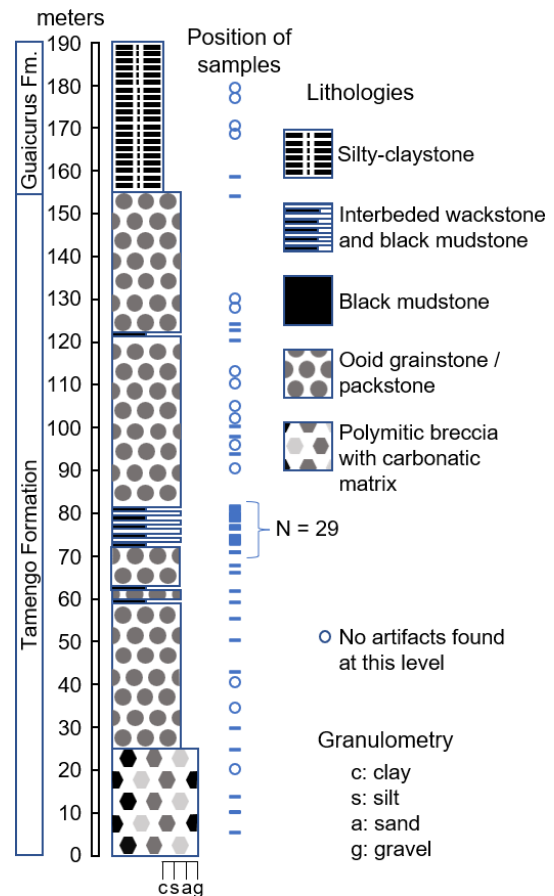


**Figure 2.** Columnar section of the Laginha quarry with stratigraphic position of samples. Modified from Amorim et al. (2020).

Initially, this methodology was adopted with the purpose of recovering mineral-walled microfossils; however, due to the extensive formation of artifacts, the remains of the original samples were submitted to another technique, replacing step 2 with the following:

- Place 200 g of these fragments in a beaker and cover it with deionized water. Place the beaker on a hot plate at 100 °C for 1 h, repeating this process for 1 week. With this methodological alteration, it would be possible to assess whether the formation of artifacts was related to the use of hydrogen peroxide.

After optical description, 10 artifacts were selected for the following analyses:

7. *Raman spectrometry*. This was used for identifying the mineralogical or molecular composition of artifacts. These analyses were carried out at the Brazilian Research Unit of Astrobiology (NAP/AstroBio) using a Renishaw inVia micro-Raman, with a laser excitation wavelength of 785 nm, 1 % power, an acquisition time of 1 s and 30 accumulations.

8. *Scanning electron microscopy with energy dispersive X-ray analyzer (SEM/EDX)*. The artifacts were covered with carbon and analyzed in order to characterize their ultrastructure and elemental composition. These analyses were carried out in the Laboratory of Scanning Electron Microscopy at the Institute of Geosciences of USP using a LEO 440 scanning electron microscope coupled with an Oxford energy dispersive X-ray spectrometer.

## 4 Results

### 4.1 Optical and electronic microscopy

The samples collected from the Tamengo Formation correspond to the following facies: carbonatic breccias, ooid grainstones (Fig. 3a), bioclastic wackestones (Fig. 3b) and carbonaceous mudstones (Fig. 3c). The sampled facies from the Guaicurus Formation correspond to siltstones and claystones, with lenses of marls. None of the thin section of any of these facies presents structures similar to those described here as artifacts.

The artifacts were only formed in samples that reacted with  $H_2O_2$ , although they did not form in all of them; in samples without pyrite, no artifacts were formed. Artifacts were formed in samples containing pyrite from both the carbonatic facies from the Tamengo Formation and the terrigenous facies from the Guaicurus Formation. In both formations, pyrite occurs, disseminated with organic matter and as isolated grains with cubic or framboid habits (Fig. 3d). In samples of black mudstone (which feature the greater concentration of pyrite), the artifacts are common (more than one artifact per 2 g of sample), and they accumulate in the granulometric fraction between 100 and 53  $\mu\text{m}$ .

The artifacts show the most varied forms, which can be grouped into three main types: (I) chambers, from which one or more tubes – open at their distal end – emerge (Fig. 4a); (II) cylinders, funnels and cones open at one or both ends (Fig. 4b–h); and (III) a set of tubes open at one end and adhered by the other to a common irregular surface or crust (Figs. 4i; 5a). These tubes, whether they are connected to a chamber (type I), isolated (type II) or connected to a crust (type III), can be straight or curved; with or without annulations on their outer surface; and with constant or variable diameters (Fig. 5b–e). Their length varies between 90 and 311  $\mu\text{m}$ , and their external diameter varies between 15 and 202  $\mu\text{m}$ .

The bioclasts found in thin sections from the Tamengo Formation correspond to tubular forms, mostly identified as cloudinids. The *Cloudina* tubes present external diameters ranging from 0.25 to 2.8 mm, wall thicknesses between 14 and 450  $\mu\text{m}$ , and lengths varying from 1.5 to 3.0 mm. The walls of these tubes are composed of calcite, with microspatic to micritic textures. In the cross-section, the walls are composed of more or less concentric circular laminae that are of varying thickness and that sometimes do not complete

the entire circumference of the tube (Fig. 3b). None of the tubular bioclasts observed in the thin section were recovered through the disaggregation techniques of the hand samples, either with the use of  $H_2O_2$  or with immersion in water and heating.

### 4.2 Energy dispersive X-Ray analysis

Under the SEM, 21 EDX analyses were obtained in 10 artifacts, and they revealed that the four major elements presented in the tubes were Fe, O, Ca and P, with mean weight percentages of 35.63 %, 34.82 %, 11.65 % and 10.28 %, respectively (Table 1). These are the only elements that appear in percentages above 1 % in all artifacts.

In some artifacts (Fig. 6a), it is possible to notice that the tube emerges from a cubic chamber that is richer in Fe and S than the tube, indicating the possibility that this portion of the artifact was previously occupied by a pyrite grain that was oxidized by the hydrogen peroxide. In higher magnification, none of the tubes show crystalline habits, being composed of an amorphous-looking material (Fig. 6b).

### 4.3 Raman spectrometry

A total of 6 of the 10 artifacts visualized by SEM were also subjected to Raman spectrometry (before carbon coating of samples). By using laser power of 10 %, the area of the artifacts hit by the laser beam completely burned, leaving a hole in the artifacts' walls (Fig. 7a), and no Raman spectrum was detected by the equipment. By diminishing the laser power to 1 %, there was no visual sign of damage to the artifacts (Fig. 7b–c), so the spectra presented here were obtained in this way. All the Raman analyses in the artifacts' walls reveal spectra with a fluorescence baseline. The fluorescence background masks the Raman signal, making unfeasible the appropriate characterization of the analyzed material.

In some spectra it is possible to notice some discrete peaks, for example the Raman shifts of 222 and 274  $\text{cm}^{-1}$  detected in two tubes (Fig. 7c); however, these and other peaks are not diagnostic of any mineral and are insufficient to characterize the tube material. Furthermore, peaks in these regions are not characteristic of the minerals identified in thin sections, which are calcite, quartz and pyrite and, subordinately, oxides or hydroxides, possibly hematite, magnetite, and/or goethite.

Ooids that disaggregated from the samples using hydrogen peroxide (Fig. 7d) were also subjected to Raman analysis. The spectra were obtained using the same parameters as those used in the analysis of the tubes, and they did not show a fluorescence effect. The acquired spectra allowed us to identify that the material that constitutes them is calcite (Fig. 7e). Furthermore, these ooids do not suffer visible damage when exposed to a laser beam at 10 % intensity.

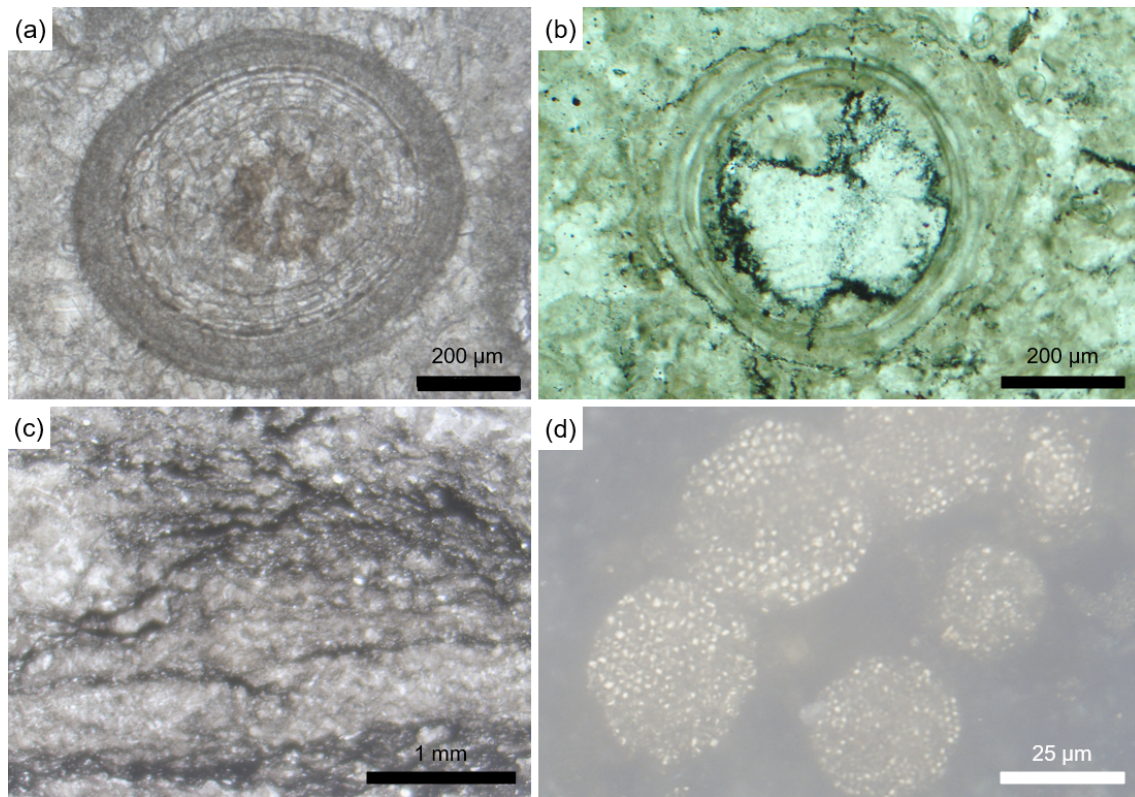


**Figure 3.** Microphotographs of thin sections from the Tamengo and Guaicurus formations. (a) Ooid grainstone, sample LAG 68.2. (b) *Cloud-ina* tube in cross-section from a bioclastic wackestone, sample LAG 74.25. (c) Carbonaceous mudstone, sample LAG 55.8. (d) Framboid pyrite grains in a claystone from the Guaicurus Formation, sample LAG 159 with reflected light. (a–c) From the Tamengo Formation with transmitted light and uncrossed polarizers.

**Table 1.** The four major elements detected by energy dispersive X-rays in 21 analyses of the artifacts' walls.

	Fe		O		Ca		P	
	Weight %	Atomic %						
Maximum value	59.01	32.19	59.01	32.19	19.91	15.08	16.37	13.50
Minimum value	18.37	7.89	18.37	7.89	4.11	3.09	2.70	2.66
Mean value	35.63	18.10	35.63	18.10	11.65	8.13	10.28	9.20
Standard deviation	10.48	6.58	10.48	6.58	4.02	2.97	3.07	2.69

## 5 Discussion

The tubular and vase-shaped structures described here were not found in thin sections, which is a strong indication that they were artifacts produced during sample preparation. In addition, none of these tubes were recovered when the samples were subjected to disaggregation without using hydrogen peroxide, indicating that this reagent is probably involved in the formation of these artifacts. This is in line with the observations of Richardson et al. (1973), who found the anellotubulates only in samples that reacted with hydrogen peroxide.

According to Pickett and Scheibnerová (1974) one of the criteria for ruling out the biological origin of anellotubulates is that their tubes are always empty. In fact, no secondary mineral is found filling the tubes; however, during laboratory preparation, they can be filled with the fine material that disintegrated from the rock, giving the false impression that it is a sedimentary filling (Fig. 5b).

The intense fluorescence emission of the material that constitutes the tubes renders Raman spectra of unfeasible interpretation. There is no record in the literature that any of the minerals commonly found in fossil remains (e.g., calcite, phosphate, quartz, pyrite, hematite) can be destroyed during Raman analysis using laser power of 10%; however, this in-

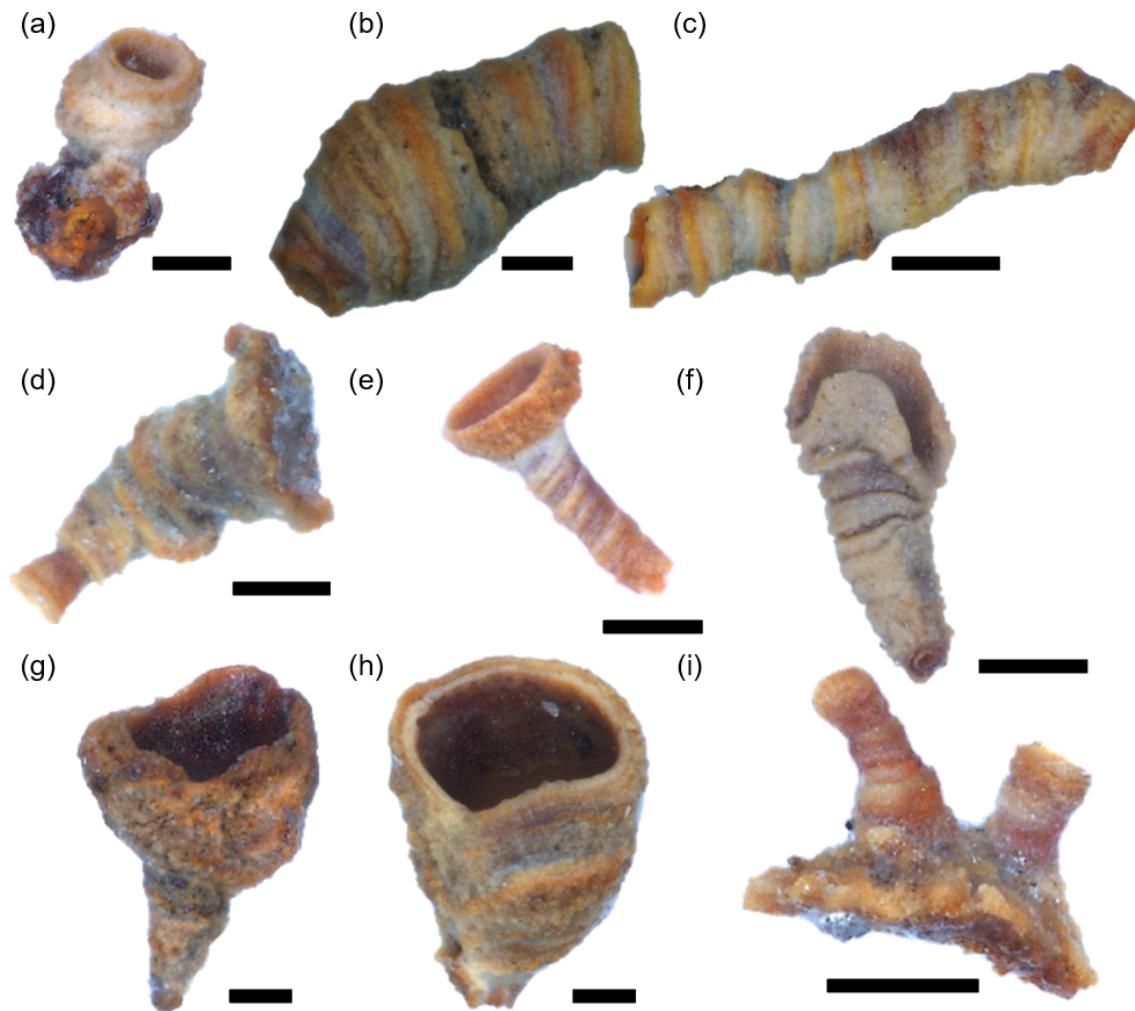


**Figure 4.** Composite-light microphotographs of pseudofossils formed by reaction between hydrogen peroxide and pyrite in samples from the Tamengo Formation. (a) Small tube connected to an irregularly shaped chamber. (b–h) Tubes varying in format from cylindrical to funnel-like and conical. (i) Tubes emerging from an irregular surface or crust. Artifacts in (a) are from sample LAG 82.00; artifacts in (b) are from LAG 74.75; artifacts in (c, h, i) are from LAG 75.05; artifacts in (d) are from LAG 81.10; artifacts in (e) are from LAG 75.50; and artifacts in (f, g) are from LAG 75.05. All scale bars are equal to 50  $\mu\text{m}$ .

formation alone is not sufficient to state that the artifacts do not have any mineral component.

SEM/EDX analysis, on the other hand, provided more conclusive results. Through SEM, it was possible to verify that the material that makes up the walls of the tubes does not have a visible crystalline habit. X-ray diffractometry conducted by McLachlan (1973) revealed that the artifacts do not have a crystalline structure, agreeing with the result presented here and reinforcing the interpretation that the tubes are not composed of a geological material. Through EDX, it was possible to characterize the elemental composition of these artifacts, which is (in mean weight percentage) iron (35.63%), oxygen (34.82%), calcium (11.65%) and phosphorous (10.28%).

Chemical analysis from anellotubulates by Pickett and Scheibnerová (1974) showed that their main components (in

weight percentage) are Fe (23.9%) and P (12.5%). Accordingly, qualitative data of electron microprobe analysis conducted by McLachlan (1973) showed that Fe and P are the main components of anellotubulates. The EDX data reported here reveal that O and Ca are also important constituents (mean weight percentage of 34.82% and 11.65%, respectively) of the tubes. Oxygen was tested by neither McLachlan (1973) nor Pickett and Scheibnerová (1974). This element may, theoretically, be present in the tubes in the form of oxides or hydroxides, phosphate, carbonate, or even water molecules incorporated into the structure of these tubes.

Calcium was detected with a weight percentage of 0.20% in the tubes analyzed by Pickett and Scheibnerová (1974) and with minor concentrations to trace in the analyses of McLachlan (1973). A possible explanation for the enormous difference between the calcium content of the tubes ana-

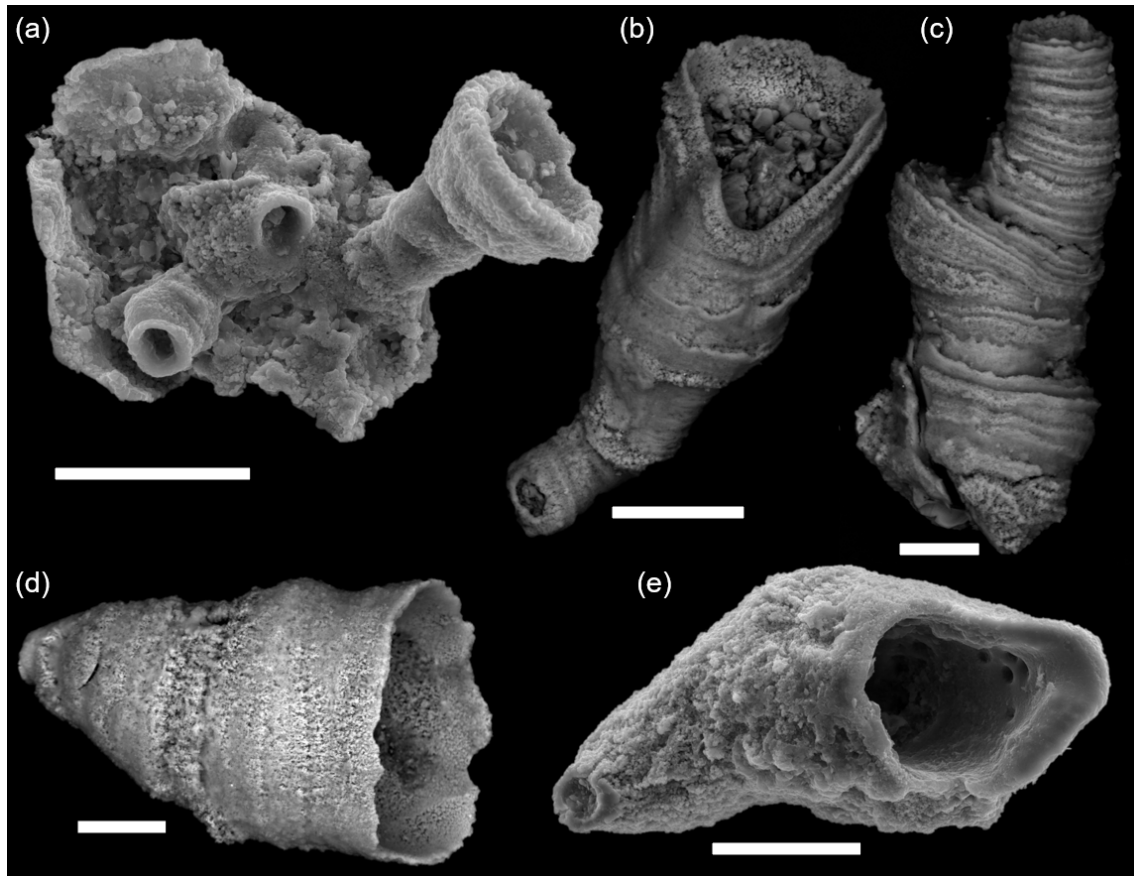


**Figure 5.** Scanning electron microscopy images of pseudofossils formed by reaction between hydrogen peroxide and samples containing pyrite. (a) Tubes emerging from an irregular surface or crust, sample LAG 76.85. (b) Tube with irregularly shaped cross-section, sample LAG 158.60. (c) Tube with varying diameter and pronounced annulations, sample LAG 75.05. (d) Tube with conical shape, sample LAG 158.60. (e) Tube with irregularly shaped cross-section and no annulations, sample LAG 159.1. (b–d) Back-scattered electron detector. (a, e) Secondary electron detector. All scale bars are equal to 50  $\mu\text{m}$ .

lyzed in this work and the tubes analyzed by Pickett and Scheibnerová (1974) is that the tubes studied by these authors were formed from the reaction of isolated pyrite grains with commercial  $\text{H}_2\text{O}_2$ , whereas in this work this reagent was added to sedimentary rocks containing pyrite grains – and most of these rocks are carbonates. The small amount of Ca in McLachlan's tubes (1973), when compared to the amount detected in the artifacts described here, can be explained, similarly, by the fact that this element is not present in large amounts in the rock samples processed by McLachlan (1973), which consisted, for the most part, of siliciclastic sediments from the Karroo Supergroup (McLachlan, 1973).

The Ca detected in the artifacts described here possibly originates from calcite grains that disaggregated from the rock and were incorporated into the tubes during their precipitation. Calcite was the only mineral containing calcium identified in the thin sections of the samples, and since this mineral does not react with  $\text{H}_2\text{O}_2$ , it is plausible to argue that Ca is present in the artifacts in the form of  $\text{CaCO}_3$  and not in other forms, such as  $\text{Ca}_3(\text{PO}_4)_2$  or CaO, for example.

According to Pickett and Scheibnerová (1974), the main component of the tubes is ferric phosphate, possibly in a hydrated form.  $\text{FePO}_4$  precipitation possibly follows the following steps:  $\text{H}_2\text{O}_2$  promotes oxidation of pyrite ( $\text{FeS}$ ), releasing ions of  $\text{Fe}^{2+}$ , which is also oxidized, and becoming  $\text{Fe}^{3+}$ , available to bond to  $\text{PO}_4^{3-}$ , present in the formulation of commercial hydrogen peroxide. Thus, iron phosphate precipitates around the pyrite grains and along the chains of bubbles released during the chemical reaction, forming the artifacts.

The presence of phosphorus is essential for the formation of artifacts, given that this element was detected in all tubes – both those analyzed in this work and those reported in the literature (McLachlan, 1973; Pickett and Scheibnerová, 1974). However, in none of the rock samples studied here was apatite or any other mineral containing phosphorus found, so the only possible source of this element is commercial hydrogen peroxide. The reagent used in this study contains, according to the manufacturer's label, 0.05 %  $\text{PO}_4^{3-}$ .

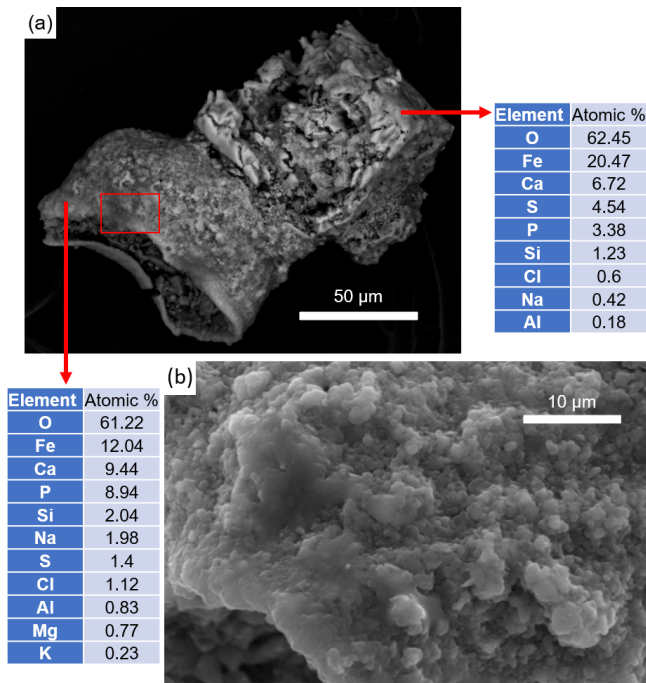


**Figure 6.** Secondary electron microscopic analyses of an artifact from the Tamengo Formation. **(a)** Back-scattered electron image of a tube with an open end and a nearly cubic termination. Arrows indicate local of energy dispersive X-ray analyses and corresponding chemical composition. **(b)** Detail image of rectangle in **(a)** with secondary electron detector. Sample LAG 62.60. Scale bars in **(a)** = 50  $\mu\text{m}$  and in **(b)** = 10  $\mu\text{m}$ .

The difficulty in identifying the artifacts is because their morphology resembles that of some bona fide fossils, such as cloudinids (Ediacaran) and some small shelly fossils (Cambrian). In the case of the artifacts described in the Tamengo Formation (this work), in which the occurrence of cloudinids is widely reported (Gaucher et al., 2003; Adorno et al., 2017; Amorim et al., 2020), special attention is required. This is because both cloudinid tubes and artifact tubes can share common characteristics, such as a more or less sinuous shape, walls formed by multiple layers, and external surfaces with equally or irregularly spaced annulations. These features can be observed in the artifacts illustrated here (Figs. 4b–c, 5b–c, 7a–b, 8a–b) and in the cloudinids described and illustrated by Germs (1972, pl. 1), Hua et al. (2005, fig. 1a–f) and Cai et al. (2014, fig. 7; 2017, figs. 4, 6).

The difference between artifacts and cloudinids is that the latter can be found in thin sections, while artifacts never appear that way, in addition to the different composition and size range (Table 2). The cloudinid tubes from the Tamengo Formation are composed of  $\text{CaCO}_3$  in the form of calcite (Gaucher et al., 2003), and cloudinids from other geological units around the globe may still be preserved through phosphatization and silicification (Cai et al., 2017). On the other hand, artifacts are constituted by a non-geological ma-

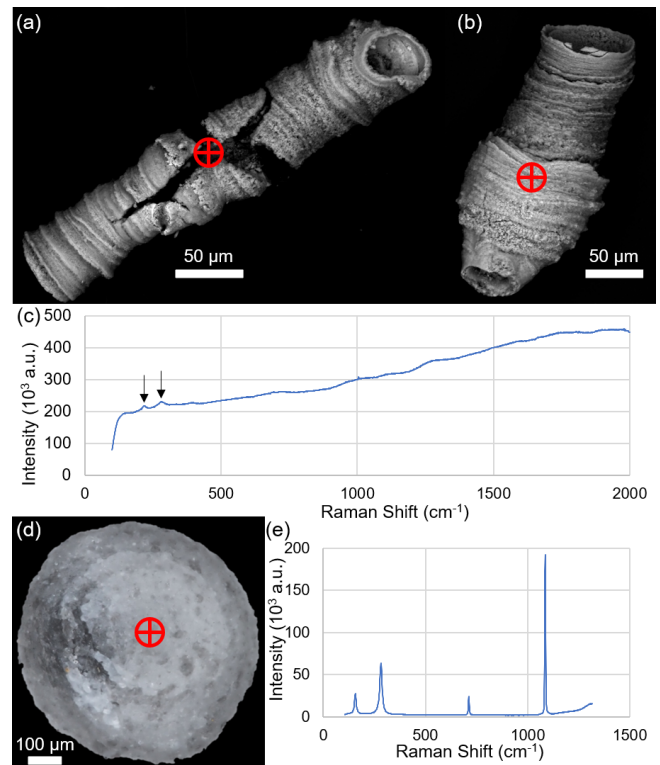


**Figure 7.** Raman analyses of artifacts and an ooid from the Tamengo Formation. Encircled crosses indicate the local hit by the laser beam during Raman analysis. **(a)** Artifact damaged by laser beam intensity of 10%, sample LAG 75.50. **(b)** Artifact hit by laser beam intensity of 1%, sample LAG 74.75. **(c)** Raman spectrum of point indicated in **(b)**; arrows indicate Raman shifts of 222 and 274  $\text{cm}^{-1}$ . **(d)** Ooid, sample LAG 28.5. **(e)** Raman spectrum of point indicated in **(d)**, discriminative of calcite. **(a, b)** SEM images acquired with back-scattered electron detector. **(d)** Microphotography under stereoscopic microscopic and reflected light.

terial containing iron and phosphorous. Regarding the size, the cloudinids found in this work have an external diameter of 0.25 to 2.8 mm and a length of 1.5 to 3.0 mm, while the cloudinid-like artifacts have an external diameter of 15 to 202  $\mu\text{m}$  and a length varying from 90 to 311  $\mu\text{m}$ . Therefore, all cloudinids found in the samples studied in this work are larger than the artifacts formed in these same samples.

Some artifacts (Fig. 8c) can also assume forms similar to vase-shaped microfossils, which requires attention since this type of microfossil can also occur in rocks of the same age as those studied in this work. These vase-shaped artifacts have the same composition as the tube-shaped artifacts and also do not occur in the thin section. The total length of these artifacts varies between 95 and 128  $\mu\text{m}$ . Most vase-shaped microfossils from the late Ediacaran have walls of carbonatic composition, although some specimens have also been preserved through silicification, phosphatization and pyritization (Chai et al., 2021). They commonly have pyriform to globose tests with constricted necks, and their total test length ranges from

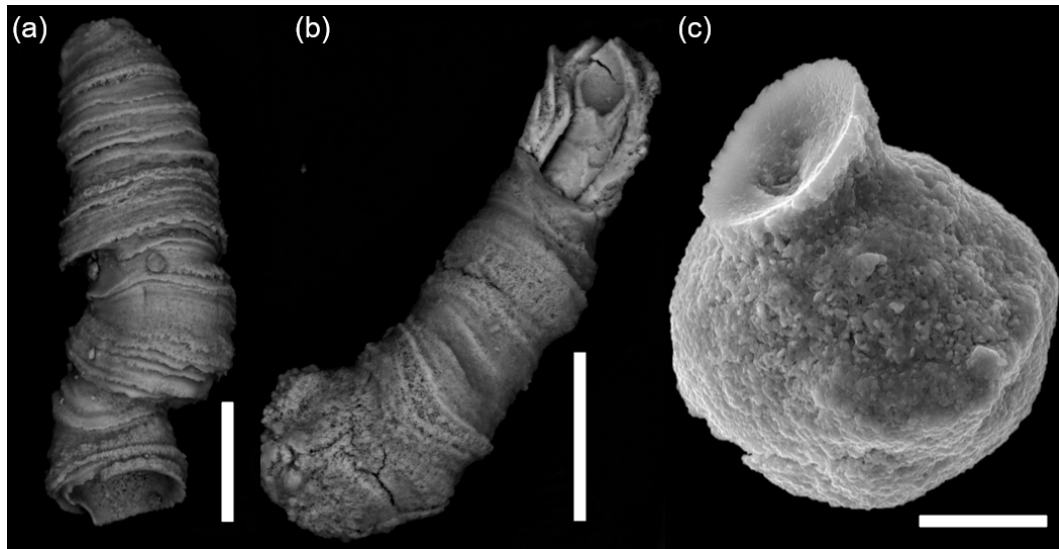


**Figure 8.** Scanning electron microscopic images of artifacts. **(a–b)** Artifacts that resemble cloudinid tubes, sample LAG 75.05, Tamengo Formation, back-scattered electron detector. **(c)** Artifact that resembles a vase-shaped microfossil, sample LAG 158.60, Guaicurus Formation, secondary electron detector. Scale bars in **(a)** and **(b)** = 50  $\mu\text{m}$  and in **(c)** = 20  $\mu\text{m}$ .

**Table 2.** Differences between cloudinids and the artifacts found in this work.

	Artifacts	Cloudinids
Can be found in thin section?	No	Yes
Length	90–311 $\mu\text{m}$	1.5–3.0 mm
Diameter	15–202 $\mu\text{m}$	0.25–2.8 mm
Elemental composition	Fe, P, Ca, O	Ca, C, P, Si, O
Mineralogy	Absent (amorphous material)	Calcite, apatite, opal
Morphology	Cylinders, funnels and cones, isolated or connected to a crust or to a chamber	Nearly cylindrical

0.1 to 3.6 mm (Hua et al., 2010; Cortijo et al., 2015; Chai et al., 2021). Therefore, vase-shaped microfossils are distinguished from similarly shaped artifacts by the same criteria that differentiate tube-shaped artifacts from cloudinids: composition, size and occurrence in the thin section.

Notwithstanding the risk of forming artifacts, the use of hydrogen peroxide in micropaleontological studies does not have to be abolished. In studies where the objective is only to analyze a particular taxon (such as Ostracoda and Foraminifera, for example), the eventual formation of artifacts would not be a cause of concern as it would be possible to identify the fossils of interest and ignore the formation of pseudofossils. Furthermore, the occurrence of these fossils can always be verified in the thin section.

Carmo (1998), who studied ostracods from the Lower Cretaceous (Potiguar Basin, Brazil), also recovered artifacts similar to those described here and concluded that they were formed by pyrite oxidation. However, other authors have recognized this type of material as fossil, indicating that the use of  $\text{H}_2\text{O}_2$  in taxonomic studies can indeed lead to misinterpretations. In addition to the aforemen-

tioned works of Wetzel (1959, 1961, 1967) and MacLachlan (1973), who described the tubular artifacts as *Anellotubulata*, Perch-Nielsen (1975), who studied core sediments of Paleocene to Eocene ages, described these tubes as incertae sedis microfossils and Keupp and Mutterhose (1994), who studied calcareous microfossils from the Lower Cretaceous (NW German basin), described these tubes as a new genus of foraminifer: *Choanaella*. However, soon after, they recognized them as artifacts (Keupp and Mutterhouse, 1995).

Particularly in the case of Precambrian and Cambrian paleobiological surveys – in which artifacts can be confused with skeletal fossils – it is preferable to avoid the use of hydrogen peroxide and opt for other rock disaggregation techniques, such as soaking in heated water, ultrasonic baths, dissolution in low-concentration acids, etc. (Harris and Sweet, 1989). Hypothetically, in the case of works that have used hydrogen peroxide in sample preparation, if there is doubt about the biogenicity of the described specimens, it is possible to re-evaluate this material through non-destructive techniques, such as SEM/EDX, and thus to identify whether they are artifacts or not.

## 6 Conclusions

Artifacts formed by the reaction between hydrogen peroxide and samples containing pyrite can strongly resemble incertae sedis tubes (e.g., cloudinids) and vase-shaped microfossils described in the Ediacaran and Cambrian systems. Due to the stratigraphic and paleobiological importance of these fossils, special attention is required for differentiating bona fide fossils from pseudofossils.

In samples treated with hydrogen peroxide, the morphological description under optical microscopes is not sufficient to separate tubular and vase-shaped fossils from the pseudofossils formed in the laboratory. Therefore, in these cases, additional analytical techniques – such as SEM/EDX – are required to support or refuse the biological origin of the studied tubes.

The SEM/EDX analyses reveal that the tubes of the pseudofossils are composed of amorphous material containing Fe, O, Ca and P. This differentiates them from mineral-walled fossils, which are composed of calcite, apatite, opal, pyrite, etc. (Table 2).

**Data availability.** The data that support the findings of this study are available at <https://doi.org/10.5061/dryad.ns1rn8q00> (Toniolo, 2023).

**Author contributions.** TFT performed the investigation, methodology and original draft preparation. JML and DAC provided supervision. TRF and LM contributed to the conceptualization. RIFT provided the resources. All the authors contributed to the review process.

**Competing interests.** The contact author has declared that none of the authors has any competing interests.

**Disclaimer.** Publisher's note: Copernicus Publications remains neutral with regard to jurisdictional claims in published maps and institutional affiliations.

**Acknowledgements.** We are grateful to Evandro Pereira da Silva for the assistance with the Raman analysis and to Isaac Jamil Sayeg for the assistance with the SEM/EDX analysis.

**Financial support.** This study was financed by the São Paulo Research Foundation (FAPESP; process no. 2016/06114-6). Thiago F. Toniolo received a scholarship from the Conselho Nacional de Desenvolvimento Científico e Tecnológico (CNPq; process no. 141861/2019-3).

**Review statement.** This paper was edited by Luke Mander and reviewed by Wilson Taylor and one anonymous referee.

## References

- Adorno, R. R., Carmo, D. A., Germs, G., Walde, D. H., Denezine, M., Boggiani, P. C., Silva, S. C. S., Vasconcelos, J. R., Tobias, T. C., Guimarães, E. M., Vieira, L. C., Figueiredo, M. F., Moraes, R., Caminha, S. A., Suarez, P. A. Z., Rodrigues, C. V., Caixeta, G. M., Pinho, D., Schneider, G., and Muyamba, R.: *Cloudina luciano* (Beurlen & Sommer, 1957), Tamengo Formation, Ediacaran, Brazil: taxonomy, analysis of stratigraphic distribution and biostratigraphy, *Precambrian Res.*, 301, 19–35, <https://doi.org/10.1016/j.precamres.2017.08.023>, 2017.
- Amorim, K. B., Afonso, J. W. L., Leme, J. M., Diniz, C. Q. C., Rivera, L. C. M., Gómez-Gutiérrez, J. C., Boggiani, P. C., and Trindade, R. I. F.: Sedimentary facies, fossil distribution and depositional setting of the late Ediacaran Tamengo Formation (Brazil), *Sedimentology*, 67, 3422–3450, <https://doi.org/10.1111/sed.12749>, 2020.
- Boggiani, P. C., Gaucher, C., Sial, A. N., Babinski, M., Simon, C. M., Riccomini, C., Ferreira, V. P., and Fairchild, T. R.: Chemostratigraphy of the Tamengo Formation (Corumbá Group, Brazil): a contribution to the calibration of the Ediacaran carbon-isotope curve, *Precambrian Res.*, 182, 382–401, <https://doi.org/10.1016/j.precamres.2010.06.003>, 2010.
- Cai, Y., Hua, H., Schiffbauer, J. D., Sun, B., and Yuan, X.: Tube growth patterns and microbial mat-related lifestyles in the Ediacaran fossil *Cloudina*, Gaojiashan Lagerstätte, South China, *Gondwana Res.*, 25, 1008–1018, <https://doi.org/10.1016/j.gr.2012.12.027>, 2014.
- Cai, Y., Cortijo, I., Schiffbauer, J. D., and Hua, H.: Taxonomy of the late Ediacaran index fossil *Cloudina* and a new similar taxon from South China, *Precambrian Res.*, 298, 146–156, <https://doi.org/10.1016/j.precamres.2017.05.016>, 2017.
- Campanha, G. A., Boggiani, P. C., Sallun Filho, W., de Sá, F. R., Zuquim, M. D. P. S., and Piacentini, T.: A faixa de dobramento Paraguai na Serra da Bodoquena e depressão do Rio Miranda, Mato Grosso do Sul. *Geol. USP Sér. cient.*, 11, 79–96, <https://doi.org/10.5327/Z1519-874X2011000300005>, 2011.
- Carmo, D. A.: Taxonomia, paleoecologia e distribuição estratigráfica dos ostracodes da Formação Alagamar (Cretáceo Inferior), bacia Potiguar, Brasil, PhD dissertation, Universidade Federal do Rio Grande do Sul, 155 pp., 1998.
- Chai, S., Hua, H., Ren, J., Dai, Q., and Cui, Z.: Vase-shaped microfossils from the late Ediacaran Dengying Formation of Ningqiang, South China: taxonomy, preservation and biological affinity, *Precambrian Res.*, 352, 105968, <https://doi.org/10.1016/j.precamres.2020.105968>, 2021.
- Cortijo, I., Mus, M. M., Jensen, S., and Palacios, T.: Late Ediacaran skeletal body fossil assemblage from the Navalpino anticline, central Spain, *Precambrian Res.*, 267, 186–195, <https://doi.org/10.1016/j.precamres.2015.06.013>, 2015.
- Denezine, M., Adorno, R. R., Carmo, D. A., Guimarães, E. M., Walde, D. H. G., Alvarenga, C. J. S., Germs, G., Antonietto, L. S., Rodríguez, C. G. V., and Nunes Junior, O. O.: Methodological development on preparation for micropaleontological and sedimentological studies based on Proterozoic record, *Front. Earth*

- Sci., 10, 810406, <https://doi.org/10.3389/feart.2022.810406>, 2022.
- Diniz, C. Q., Leme, J. M., and Boggiani, P. C.: New species of macroalgae from Tamengo Formation, Ediacaran, Brazil, *Front. Earth Sci.*, 9, 748876, <https://doi.org/10.3389/feart.2021.748876>, 2021.
- Gaucher, C., Boggiani, P. C., Sprechmann, P., Sial, A. N., and Fairchild, T.: Integrated correlation of the Vendian to Cambrian Arroyo del Soldado and Corumbá Groups (Uruguay and Brazil): palaeogeographic, palaeoclimatic and palaeobiologic implications, *Precambrian Res.*, 120, 241–278, [https://doi.org/10.1016/S0301-9268\(02\)00140-7](https://doi.org/10.1016/S0301-9268(02)00140-7), 2003.
- Germis, G. J.: New shelly fossils from Nama Group, south west Africa, *Am. J. Sci.*, 272, 752–761, <https://doi.org/10.2475/ajs.272.8.752>, 1972.
- Harris, A. G. and Sweet, W. C.: Mechanical and chemical techniques for separating microfossils from rock, sediment and residue matrix, *Paleontological Society Special Publications*, 4, 70–86, <https://doi.org/10.1017/S2475262200005013>, 1989.
- Hua, H., Chen, Z., Yuan, X., Zhang, L., and Xiao, S.: Skeletogenesis and asexual reproduction in the earliest biomineralizing animal Cloudina, *Geology*, 33, 277–280, <https://doi.org/10.1130/G21198.1>, 2005.
- Hua, H., Chen, Z., Yuan, X., Xiao, S., and Cai, Y.: The earliest foraminifera from southern Shaanxi, China, *Sci. China Earth Sci.*, 53, 1756–1764, <https://doi.org/10.1007/s11430-010-4085-x>, 2010.
- Keupp, H. and Mutterlose, J.: Calcareous phytoplankton from the Barremian/Aptian boundary interval in NW Germany, *Cretaceous Res.*, 15, 739–763, <https://doi.org/10.1006/cres.1994.1040>, 1994.
- Keupp, H. and Mutterlose, J.: Erratum, *Cretaceous Res.*, 16, 151, <https://doi.org/10.1006/cres.1995.1011>, 1995.
- Lacerda-Filho, J. V., Brito, R. S. C., Silva, M. G., Oliveira, C. C., Moreton, L. C., Martins, E. G. Lopes, R. C., Lima, T. M., Larizatti, J. H., and Valente, C. R.: *Geologia e Recursos Minerais do Estado de Mato Grosso do Sul: texto explicativo, CPRM – Serviço Geológico do Brasil, Campo Grande, 200 pp., 1 map, 1 : 1.000.000 scale*, 2006.
- Leme, J. M., Van Iten, H., and Simões, M. G.: A New Conulariid (Cnidaria, Scyphozoa) from the Terminal Ediacaran of Brazil, *Front. Earth Sci.*, 10, 777746, <https://doi.org/10.3389/feart.2022.777746>, 2022.
- McLachlan, R. R.: Problematic microfossils from the Lower Karroo beds in South Africa, *Palaeont. Afr.*, 15, 1–21, 1973.
- Morais, L., Fairchild, T. R., Freitas, B. T., Rudnitzki, I. D., Silva, E. P., Lahr, D., Moreira, A. C., Abrahão Filho, E. A., Leme, J. M., and Trindade, R. I. F.: Doushantuo-Pertatataka – Like Acritarchs From the Late Ediacaran Bocaina Formation (Corumbá Group, Brazil), *Front. Earth Sci.*, 9, 787011, <https://doi.org/10.3389/feart.2021.787011>, 2021.
- Parry, L. A., Boggiani, P. C., Condon, D. J., Garwood, R. J., Leme, J. D. M., McIlroy, D., Brasier, M. D., Trindade, R., Campanha, G. A. C., Pacheco, M. L. A. F., Diniz, C. Q. C., and Liu, A. G.: Ich-nological evidence for meiofaunal bilaterians from the terminal Ediacaran and earliest Cambrian of Brazil, *Nat. Ecol. Evol.*, 1, 1455–1464, <https://doi.org/10.1038/s41559-017-0301-9>, 2017.
- Perch-Nielsen, K.: Eocene to Paleocene microfossil of unknown affinity, *DSDP Initial Reports*, 29, 909–911, <https://doi.org/10.2973/dsdp.proc.29.125.1975>, 1975.
- Pickett, J. and Scheibnerová, V.: The inorganic origin of “anelletotubulates”, *Micropaleontology*, 20, 97–102, <https://doi.org/10.2307/1485101>, 1974.
- Richardson, G., Gregory, D., and Pollard, J.: Anelletotubulates are manufactured “microfossils”, *Nature*, 246, 347–348, <https://doi.org/10.1038/246347a0>, 1973.
- Thomas, F. C. and Murney, M. G.: Techniques for extraction of foraminifers and ostracodes from sediment samples, *Can. Tech. Rep. Hydrogr. Ocean Sci.*, 54, 1–24, 1985.
- Toniolo, T.: Raman spectra and SEM EDX analyses of artifacts resembling Ediacaran/Cambrian fossils, *Dryad* [data set], <https://doi.org/10.5061/dryad.ns1rn8q00>, 2023.
- Wetzel, O.: New problematic microfossils from the German Upper Lias, *XV Int. Congr. Zool. London*, 50, 1060, 1959.
- Wetzel, O.: New microfossils from Baltic Cretaceous flintstones, *Micropaleontology*, 7, 337–350, 1961.
- Wetzel, O.: Rätselhafte mikrofossilien des Oberlias ( $\epsilon$ ): Neue funde von “Anelletotubulaten”, *Neues Jahrb. Geol. P.*, 128, 341–352, 1967.